JACC: CARDIOVASCULAR IMAGING

IMAGING VIGNETTE

The Impact of Integrated Non-invasive Imaging in the Management of Takayasu Arteritis

Christopher P Uy, MD,[a] Jason M Tarkin, PhD,[d] Deepa Gopalan, MRCP, FRCR,[b] Tara D Barwick, MD,[b] Enrico Tombetti, MD,[c] Taryn Youngstein, MD,[a,d] Justin C Mason, PhD,[a,d]

From the Departments of [a]Rheumatology and [b]Imaging Departments, Hammersmith Hospital, Imperial College Healthcare Trust, London, UK, [c]Department of Biomedical and Clinical Sciences 'L. Sacco', University of Milan, Milan, Italy, and [d]National Heart and Lung Institute, Imperial College, London, UK.

c.uy@nhs.net
jt545@cam.ac.uk
d.gopalan@nhs.net
tara.barwick@nhs.net
enricotombetti@gmail.com
taryn.youngstein@nhs.net
justin.mason@imperial.ac.uk

Acknowledgements
This study received infrastructure support for the Imperial College National Institute for Health Research Biomedical Research Centre, London UK. JT is supported by Wellcome Trust. There are no relationships with industry relevant to this study.

Address for correspondence:
Professor Justin Mason, National Heart and Lung Institute, Imperial College, Hammersmith Hospital, Du Cane Road, London W12 0NN, UK.
Tel: +44-20-7594-2720 Fax: +44-20-7594-3653 justin.mason@imperial.ac.uk

Rapid technological advances in non-invasive imaging, combined with their increased availability in health systems around the world, have helped transform clinical management in Takayasu arteritis (TA) and minimized the need for intra-arterial angiography. TA, a rare autoimmune granulomatous vasculitis most commonly presenting in young adulthood, predominantly affects the aorta and its major branches. The disease targets the arterial wall, where inflammatory infiltrates are comprised of T and B lymphocytes, monocytes, macrophages and giant cells. Secondary myofibroblast proliferation results in arterial stenosis and occlusion, while disruption of the medial layer predisposes to aneurysm formation. Serious sequelae include systemic and pulmonary arterial hypertension, myocardial infarction, cardiac failure, cerebral ischemia and stroke. Immunosuppressive therapy is employed to suppress inflammation, to prevent arterial injury and encourage positive remodeling. Multi-modal imaging involving magnetic resonance imaging (MRI) / angiography (MRA), computed tomography angiography (CTA), high-resolution ultrasound (US) and positron-emission tomography (PET), facilitates early diagnosis, reveals the extent and severity of arterial injury, and offers a sensitive means for monitoring treatment responses and promptly detecting signs of disease progression.

Figure 1. Identification of arterial wall inflammation.

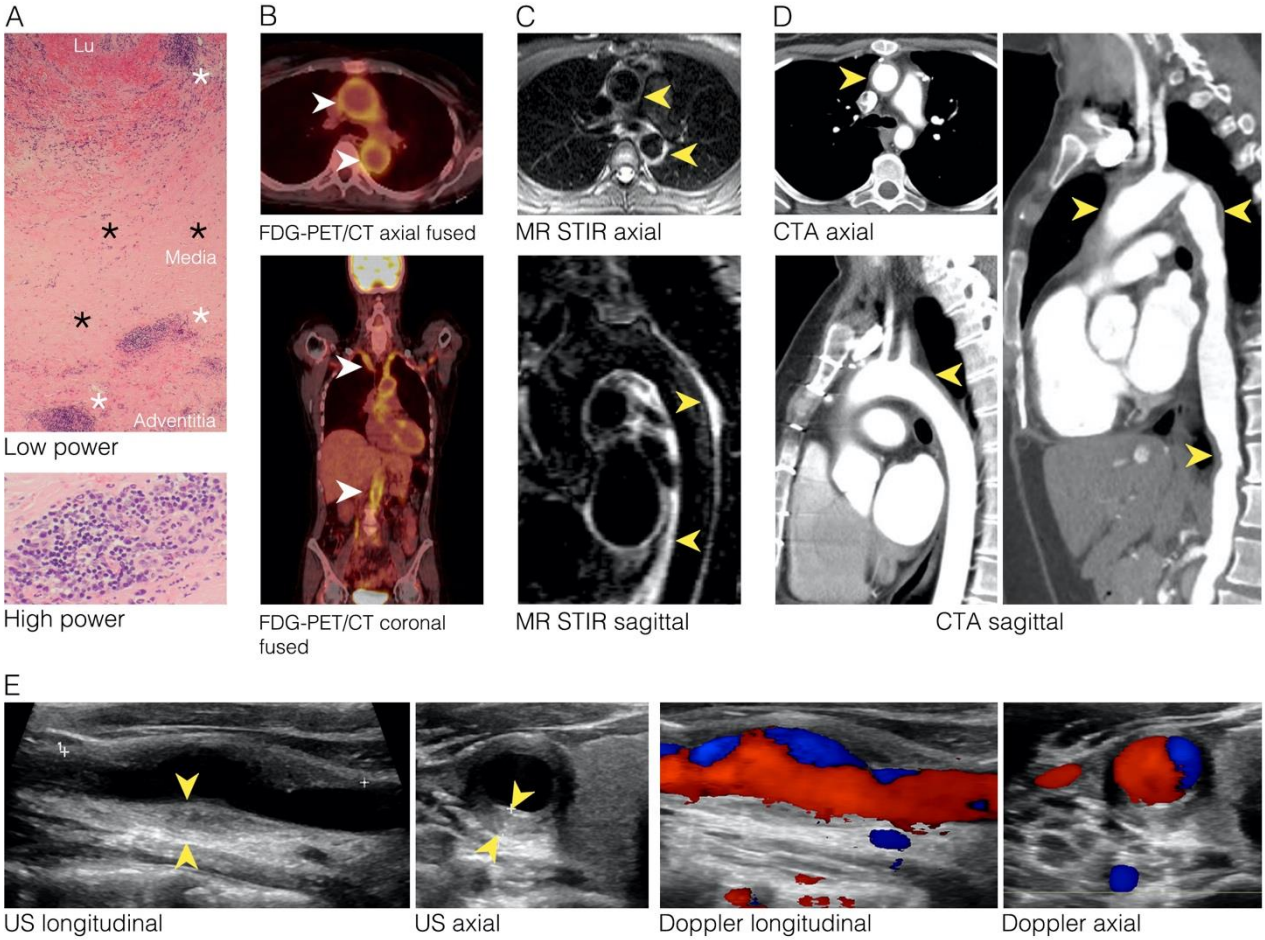

(A) This surgical specimen from the common carotid artery reveals granulomatous arteritis throughout the arterial wall from adventitia to the lumen (Lu), with discrete foci of inflammation (white asterisks), and secondary myofibroblast proliferation (black asterisks) resulting in lumen occlusion. At higher power, the dense infiltrate predominantly consists of T cells and monocytes, with multinucleate giant cell formation. Leukocytes and myofibroblasts are among the metabolically active vascular cells that take up the positron tomography ligand 2-[^{18}F]-fluoro-2-deoxy-D-glucose (FDG-PET/CT) in TA shown in **(B)**. The FDG-PET/CT imaging demonstrates intense homogenous tracer uptake throughout the vessel wall, consistent with aortitis and subclavian arteritis (arrows). FDG-PET/CT can detect active arteritis early in the disease course and before significant arterial injury. **(C)** Axial and sagittal double inversion recovery MRA sequences through the thorax demonstrates mural thickening of the ascending and descending thoracic aorta in another patient with early clinically active pre-stenotic disease (arrows). **(D)** CTA can also demonstrate active, pre-stenotic aortitis. The images reveal significant concentric thickening of the ascending aortic, distal arch and proximal descending aorta (arrows) and, in more established disease (right), additional luminal irregularity. High-resolution Doppler ultrasound (US) is a sensitive means for identifying arterial wall thickening and enhancement, in accessible vessels. **(E)** The images reveal concentric, homogenous thickening of the common carotid artery wall (Macaroni's sign; arrows) in a young patient with evidence of focal arterial wall dilatation and disturbed blood flow (colour Doppler).

Figure 2. Demonstration of disease extent and pattern.

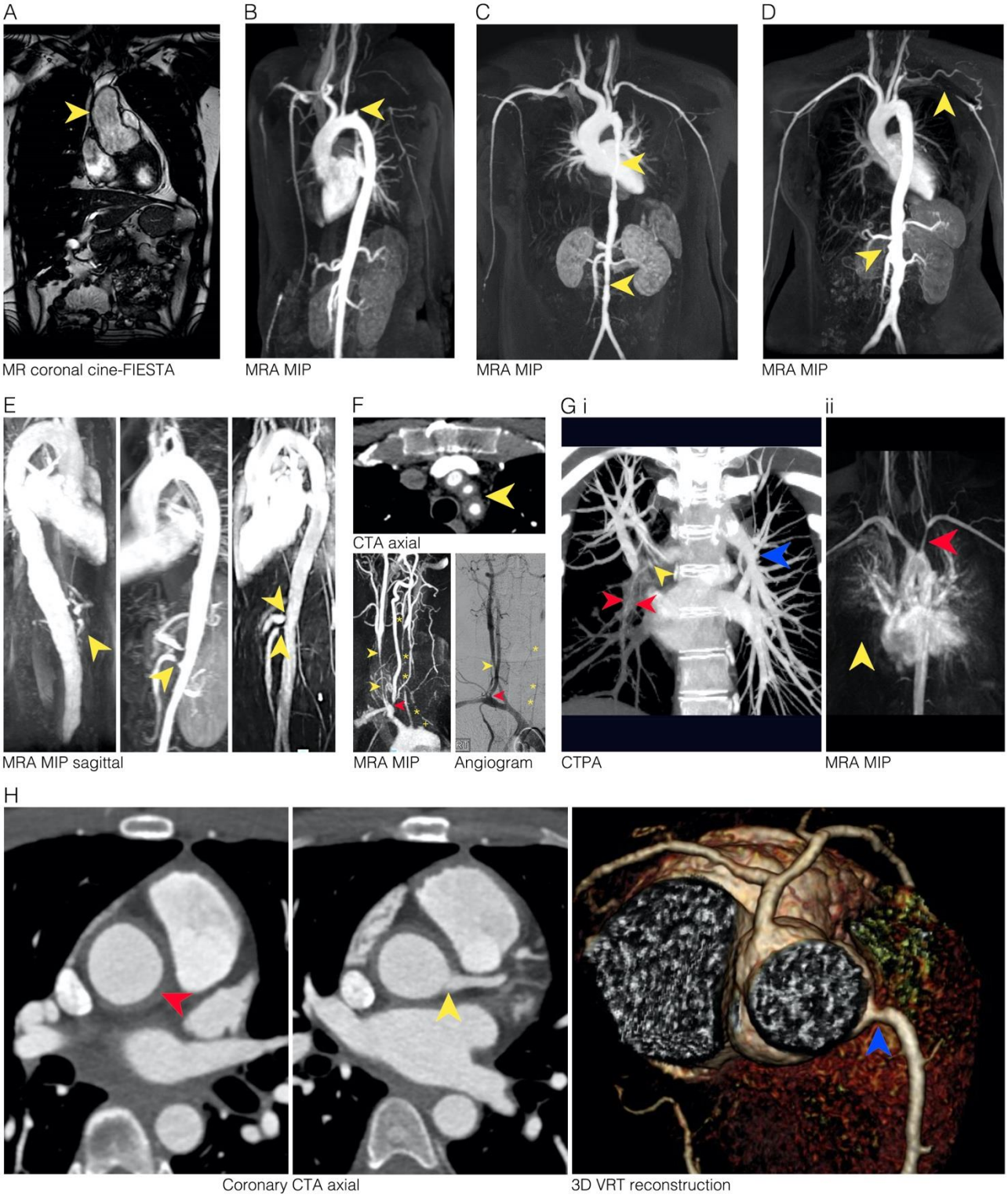

MRA offers a sensitive and readily accessible means for identifying the extent and severity of arterial injury, both at diagnosis and subsequently, to assess the efficacy of immunosuppressive therapy. The lack of ionising radiation allows serial imaging, particularly important for younger patients. Maximum intensity projection (MIP) of the MRA and volume rendering technique (VRT) of the CTA are presented.

(A) Ascending aortitis is often complicated by aortic root dilatation (arrow) and aortic valve regurgitation, which may require surgical intervention. **(B)** Subclavian artery stenosis/occlusion is a common sequelae of injury in TA, often leading to upper limb claudication. **(C)** MRA reveals the extent of injury in the thoracic and abdominal aorta. Lower limb claudication may occur secondary to significant thoracic and/or abdominal

aortic stenoses, as demonstrated. **(D)** Arterial injury may occur above and below the diaphragm. In this example, there are occlusions of the left subclavian artery and right renal artery, with distal aortic irregularity. Ischemic injury led to loss of the right kidney. Sub-diaphragmatic disease with visceral artery involvement is commonly seen. **(E)** Classical proximal arterial stenosis with post-stenotic dilatation is seen in these sagittal images affecting the coeliac axis and superior mesenteric artery. Disease affecting the supra-aortic vessels may result in cerebral ischemia and stroke. **(F)** Supra-aortic artery arteritis, with cuffing of the great vessels by inflammatory tissue is shown here by CTA. Disease may progress to widespread stenosis/occlusion, as demonstrated by the corresponding CT image, where there is involvement of the left subclavian artery (+), left common carotid artery (asterisks), right common carotid artery (yellow arrows) and right and left vertebral arteries (red arrows). The intra-arterial angiogram demonstrates a paucity of flow on the left side (asterisks), with cerebral perfusion dependent upon the right-sided circulation. Pulmonary artery involvement is seen in up to 50% of TA patients. Stenoses are more common than aneurysms. **(G)**(i) Computed tomography pulmonary angiogram (CTPA) coronal maximum intensity projection demonstrates severe stenosis of the right lower lobe pulmonary artery, with a thin central trickle of contrast medium (yellow arrow) followed by segmental occlusion. There is concentric soft tissue thickening of the arterial wall (red arrows). Comparatively, the left lower lobe pulmonary artery (blue arrow) is of normal calibre with good segmental arterial opacification. (ii) The corresponding delayed phase MR angiogram shows a large perfusion defect in the right lower lobe (yellow arrow), as well as concomitant systemic arterial involvement (left subclavian artery stenosis; red arrow). Dedicated cardiac MRI may identify pulmonary disease and help to exclude cardiac complications including myocarditis. **(H)** Coronary CTA can identify proximal vasculitic lesions in the coronary arteries (arrows). In this example, inflammatory thickening of the aortic root (red arrow) extends to involve the proximal left coronary artery (yellow arrow). 3D VRT also shows the presence of a proximal right coronary artery stenosis (blue arrow).

Figure 3. Assessment of response to treatment in Takayasu arteritis.

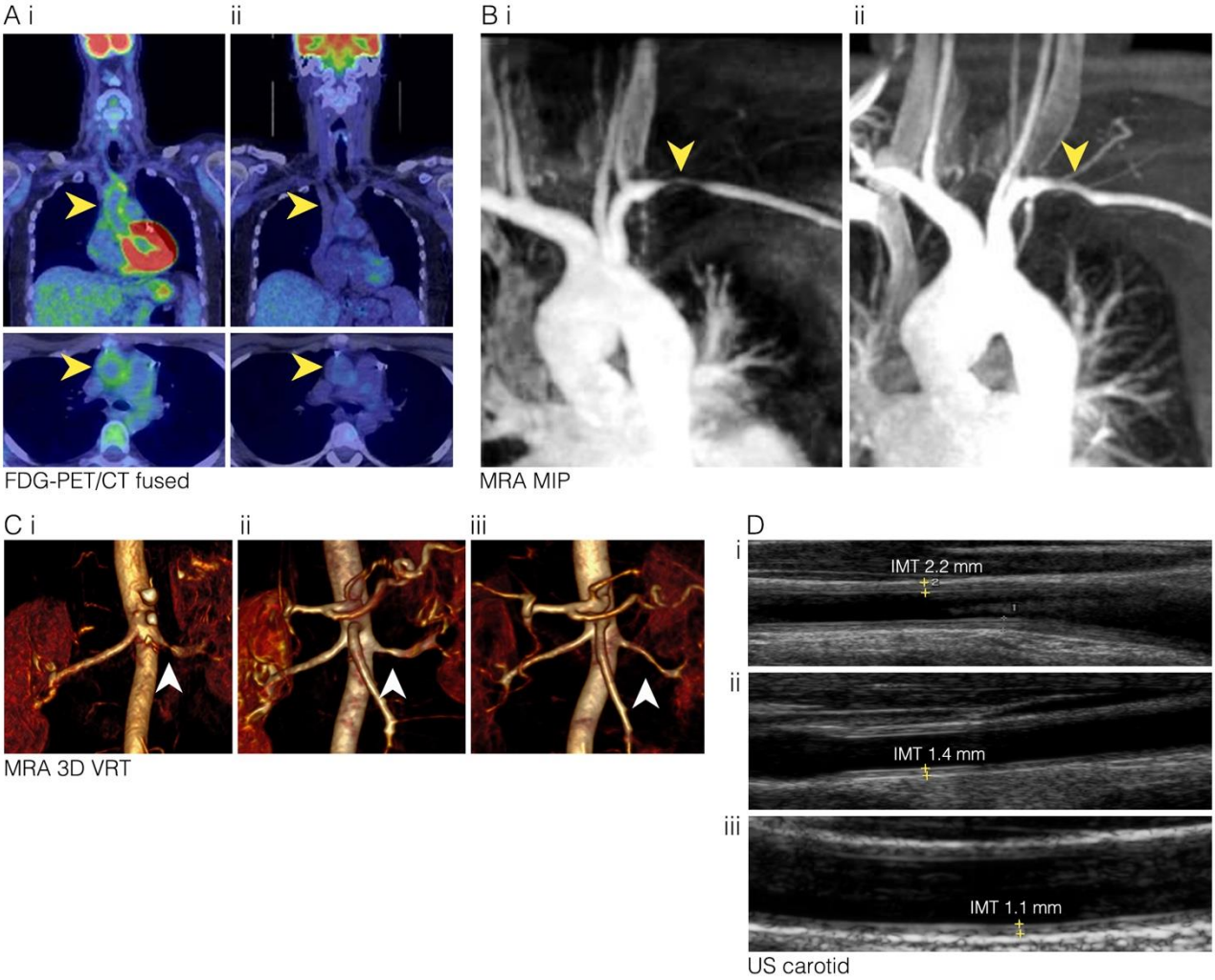

Non-invasive imaging contributes to decisions concerning changes in therapy. **(A)** Intense FDG avidity associated with active disease (arrows), was suppressed by combination immunosuppressive therapy including tocilizumab, shown in the follow-up scan six months later. The low-grade FDG uptake in the aorta likely represents mild residual disease activity (arrows). **(B)** In another patient, the MRA identified a progressing tight left subclavian artery stenosis (arrow). In response to escalation of the immunosuppressive therapy the artery remodeled with improvement in the degree of luminal stenosis 1 year later (arrow); a response that may be seen in up to 25% of lesions(1). **(C)** In this next example, the left renal artery stenosis seen on the MRA at diagnosis improved after 3 years of treatment with prednisolone and methotrexate (ii). The arterial anatomy returned to normal at 5 years (not shown) and was unchanged in the MRA 12 year's post-diagnosis, (iii) and 2 years after cessation of all therapy. **(D)** High resolution US offers a sensitive means for monitoring carotid disease. Here, increased intimal medial thickening (IMT) observed by US at diagnosis, subsequently normalized in response to therapy.

Figure 4. Monitoring of disease progression and impact

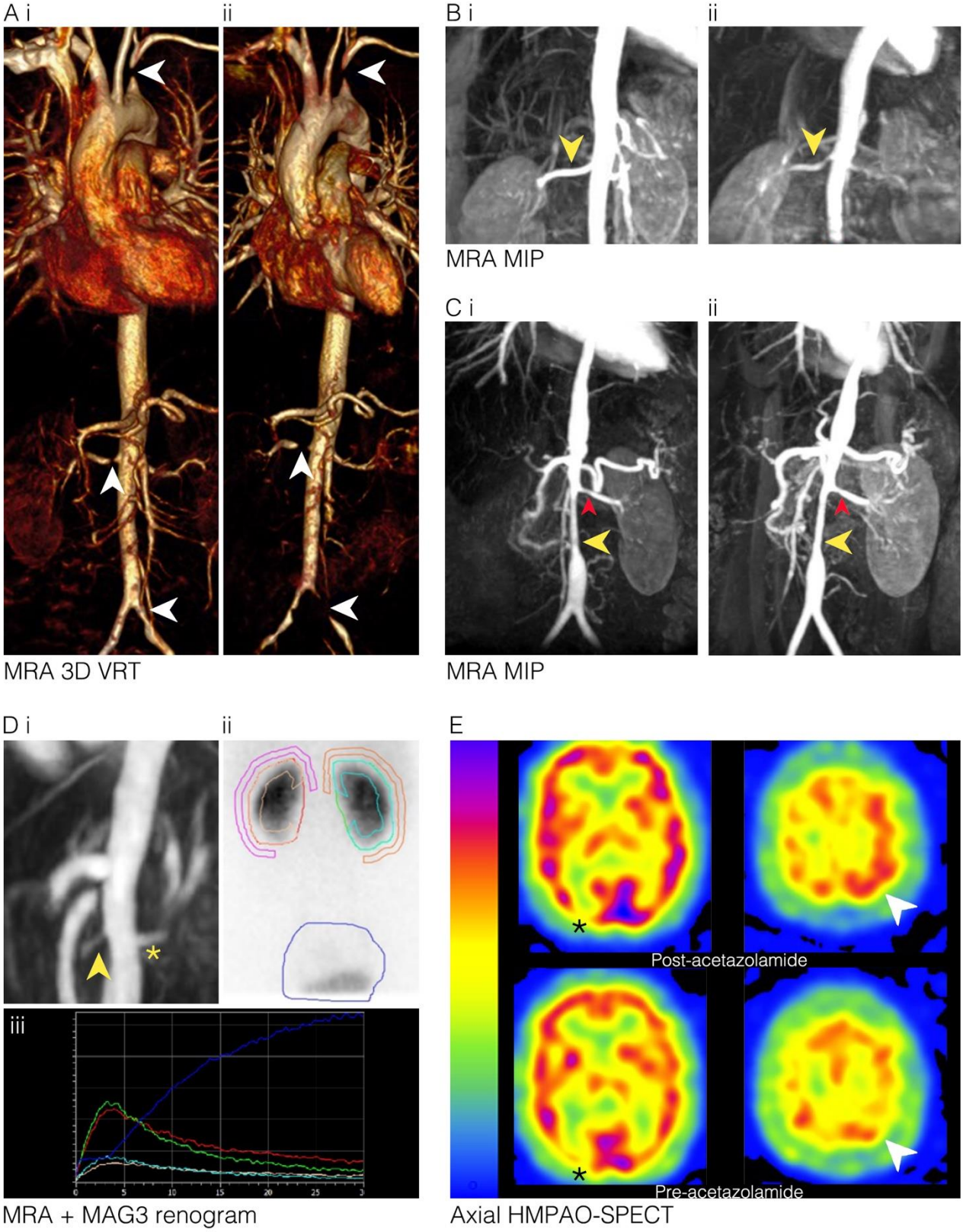

Routine interval MRA imaging is used to facilitate early detection of new or progressive arterial lesions. MRI may also reveal new or progressive wall thickening suggestive of active disease. **(A)** MRA indicates persistent stenosis in the left subclavian and right renal artery, while the changing anatomy in the left common iliac artery is consistent with progressive stenotic disease, compared to baseline imaging (arrows). **(B)** In this example, MRA reveals the development of new stenoses affecting the right and left renal arteries despite combination immunosuppressive therapy. There was no change in clinical parameters to warn of this

important disease progression, which was only detected by imaging. **(C)** Prolonged immunosuppressive therapy resulted in detectable increases in the diameter of the abdominal aortic lumen (yellow arrow) and left renal artery (red arrow). Although modest, these changes in arterial diameter are sufficient to significantly increase distal blood flow as described by Poiseuille's law. **(D)** The potential functional impact of right renal artery stenosis (arrow) versus normal left (star) can be investigated by Technetium-99m dimercapto succinic acid (Tc99m-DSMA), a static radionucleotide scan used to assess parenchymal renal function (ii and iii) before and after intervention. The contribution was left 46% and right 54% and the decision was made to optimise blood pressure control using renal artery angioplasty. **(E)** Cerebral ischemia may complicate supra-aortic TA. In this patient, 99mTc labeled hexamethylene-propyleneamine oxime (HMPAO) SPECT imaging was used to assess cerebral perfusion and the need for revascularization. The pre- (bottom row) and post- (top row) acetazolamide challenge images show expected improvement in perfusion post-acetazolamide, except at the site of an established right occipital infarct (star). The superior left frontal lobes have adequate vascular reserve and show increased perfusion post-acetazolamide (white arrow), while the right side shows no change indicating poor vascular reserve.

Figure 5. Outcomes: collateral circulation, aneurysms and intervention

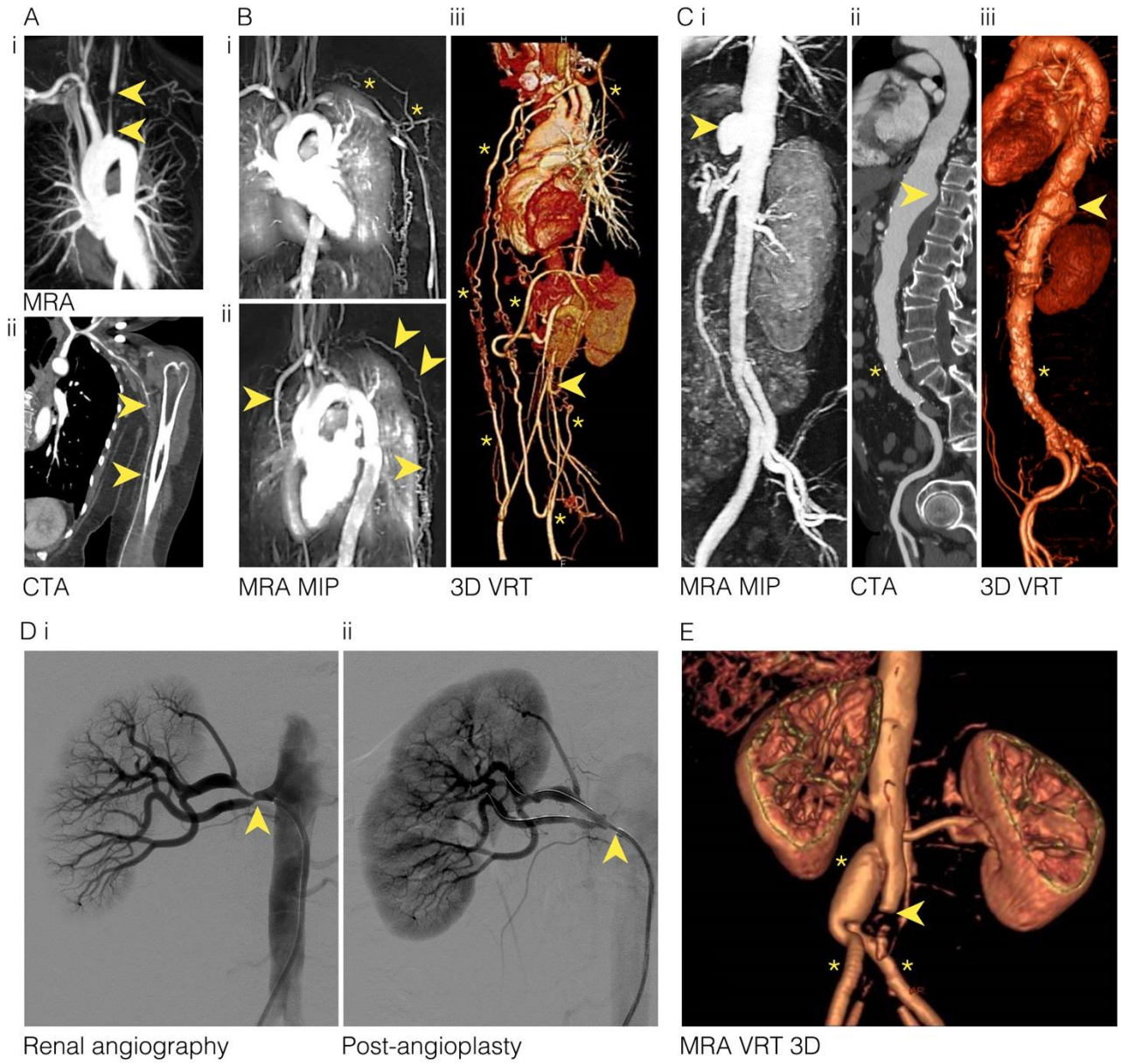

(A) Long fixed fibrotic arterial stenoses (arrows) are commonly seen in TA, as demonstrated here in the left common carotid artery (i), the left subclavian (SCA) and axillary arteries (ii). Resulting tissue ischemia may be an important driver for collateral artery formation which can significantly reduce ischemic symptoms. **(B)** The thoracic MRA in panel (i) demonstrates upper limb collaterals around a left SCA occlusion (asterisks). Panel (ii) shows long collaterals arising from mediastinal and intercostal vessels (arrows) in response to severe supra-aortic disease. In panel (iii) the 3D volume rendered reconstruction shows extensive disease of the aorta culminating in distal occlusion (arrow) and extensive collaterals (asterisks) which revascularise the gastrointestinal and the lower limb circulation. Aneurysms represent an important complication of TA. **(C)** The mid-aortic saccular aneurysm (arrow) in (i) developed following a severe disease flare and was successfully treated using an endovascular stent. CT angiography in (ii) and (iii) reveals a focal thoracic aortic aneurysm appearing later in the disease course (arrows), along with premature distal secondary atherosclerosis (asterisks). Surgical treatment is used sparingly for specific indications in TA, with both endovascular and open surgical procedures employed. **(D)** The use of digital subtraction angiography (DSA) is now predominantly confined to the preparation for arterial revascularisation (see also Figure 2F). The DSA reveals right renal artery stenosis responsible for hypertension and renal ischemia (arrows), which was treated successfully with balloon angioplasty. **(E)** Distal aortic occlusion accompanied by disabling lower limb claudication can be treated effectively with aorto-bifemoral grafting. MRA VRT 3D reconstruction shows the occluded native aorta (arrow), with an aorto-bifemoral graft anastomosed proximally (asterisks).

References

1. Tombetti, E., Godi, C., Ambrosi, A., Doyle, F., Jacobs, A., Kiprianos, A., Youngstein, T., Bechman, K., Manfredi, A., Ariff, B. and Mason, J. (2018). Novel Angiographic Scores for evaluation of Large Vessel Vasculitis. *Scientific Reports*, 8(1).